NO sensing property and adsorption behavior of $(La_{0.8}Sr_{0.2})_2FeNiO_{6-\delta}$ sensitive electrode for YSZ-based potentiometric sensor

Lihong Zhou[1, a], Junyi Lu[2, b], Duan Wei[3, c] Bikang Hu[4, d] and Jianzhong Xiao[5, e]

[1,2,3,4] City College, Wuhan University of Science and Technology, Wuhan, Hubei 430083, P. R. China

[3, 5] State Key Laboratory of Materials Processing and Die & Mold Technology, School of Materials Science and Engineering, Huazhong University of Science and Technology, Wuhan, Hubei 430074, P. R. China

[a]lihongzhou2004@163.com, [b]weixue.123456789@163.com, [c]davidjiangyi@foxmail.com, [d]qiande_huang@163.com, [e]jzxiao@mail.hust.edu.cn

Keywords: $(La_{0.8}Sr_{0.2})_2FeNiO_{6-\delta}$; Double-perovskite; NO Sensitivity; Ddsorption-desorption; YSZ.

Abstract. The $(La_{0.8}Sr_{0.2})_2FeNiO_{6-\delta}$ (LSFN) oxide powder with double-perovskite structure was prepared by using polymeric precursor method. The oxide powder and LSFN sensing electrode (LSFN-SE) were characterized by X-ray diffraction (XRD) and environmental scanning electron microscopy (ESEM). The NO sensing property of NOx potentiometric sensor based on yttria-stablized zirconia (YSZ) was investigated from 300 to 550 °C in 10 vol.% O_2. The results demonstrate that the response of the sensor with LSFN-SE sintered at 1300 °C to 600 ppm NO decreases with increasing temperature. The voltage differences of the sensor are good linear to the logarithm of NO concentrations. The NO gas adsorption-desorption behavior of the LSFN was examined. The result of NO-TPD indicates that desorption peak is not observed above 300 °C, which may be one of the reasons for the low sensitivity of NO for the LSFN.

Introduction

Mixture gases of NO and NO_2 (referred to as NOx) become serious atmospheric pollutants which give rise to photochemical smog, acid rain, ozone depletion, and greenhouse effect. Major source of NOx emission is considered from automotive exhaust, which usually contains 100-1000 ppm NOx in which 80–90 % are NO [1]. Therefore, the high-performance NOx sensors have been urgently needed to detect NOx in automobile exhaust. The NOx sensors using YSZ as oxygen ion conducting electrolytes have been widely reported [2-6].

Mixed potential type NOx sensors based on YSZ solid electrolytes have been interested in their high sensitivity, thermal stability and chemical stability. Except device structure and sensitive mechanism, many studies have focused on sensitive electrode materials [2, 7-10]. In some previous studies, many monoxides and composite oxides have been studied as SEs in YSZ-based potential type sensors. The reported monoxides were mainly NiO, WO_3, ZnO, Cr_2O_3, SnO_2, Nb_2O_5 and so on [11-15]. These monoxides provided good sensing properties for NO_2 at elevated temperatures. In particular, the nano-structured NiO reported by Miura et al. was a very excellent sensing electrode. In addition to high NO_2 sensitivity, the sensor with a NiO-SE sintered at 1100 °C showed a high selectivity to NO_2. The composite oxide is divided into spinel and perovskite. The studied spinels were $NiCr_2O_4$, $ZnFe_2O_4$, $ZnCr_2O_4$, $CrMn_2O_4$, $MnCr_2O_4$, $ZnFe_2O_4$-$ZnCr_2O_4$ and so on [2,16-18]. For a mixed potential type NOx sensor, $ZnFe_2O_4$ has been found to give the highest NOx sensitivity in the test compared to other reported spinel-type oxides. Perovskite-type composite oxides are promising SE alternatives due to their excellent NO or NO_2 catalytic properties, ease of synthesis, low cost and high thermal stability. The perovskites that have been reported to exhibit good sensing performance were $LaFeO_3$, $La_{0.8}Sr_{0.2}FeO_3$, La_2CuO_4, $(La_{0.8}Sr_{0.2})_2FeNiO_{6-\delta}$, $(La_{0.8}Sr_{0.2})_2FeMnO_{6-\delta}$ [9,10,19-23] and so on. Recently, research team of Geyu Lu reported a novel trirutile $CoTa_2O_6$ as SE. The device attached with $CoTa_2O_6$-SE sintered at 1000 °C gave the highest response of 93 mV to 100 ppm NO_2 and fast response and recovery times at 650 °C [24]. However, the electrodes of the mixed potential

type sensor generate a signal of NO2 opposite to that of NO, which leads to a complicated sensor structure design [1].

Miura et al.'s NO2-TPD results showed that the higher the amount and the peak temperature of NO2 desorption, the higher the NO2 sensitivity. The NO2 gas adsorbed strongly at the YSZ/SE interface may promote the rate of the electrochemical reaction of NO2 even at high temperatures. Therefore, it is one of the ways to improve the sensitivity of the electrode by looking for sensitive materials that can strongly adsorb NOx and the proper operating temperature [17]. Our previous results show that the double perovskite LSFN as a SE exhibits a good NO2 sensitivity at 550 -700 °C [22]. However, the sensitivity of the LSFN-SE to NO above 550 °C is small. This work expanded the sensitivity test temperature to further understand the sensitive properties of LSFN to NO, thus providing a reference for the structural design of the sensor with LSFN-SE.

In this work, NO sensitivity test is carried out for the sensor with LSFN-SE, and the NO adsorption-desorption behavior of the LSFN is studied.

Experimental

Powder Synthesis. LSFN powder was synthesized by the polymeric precursor method using La_2O_3 and nitrates of Sr, Fe and Ni [22]. Structural characterization was performed using X-ray diffraction to confirm that no additional phases, such as SrO or NiO, were present in the final powder. The LSFN powder was obtained after calcination in air at 800 °C for 10 h.

Sensor Fabrication. The configuration of sensor is shown in Fig. 1. The sintering process of the YSZ disc and the Pt reference electrode has been previously presented [22]. The LSFN-SE was sintered at 1300 °C for 1 h in air. Finally, Ag paste (Synthetic Resin Institute of Shanghai, China) of the shape shown in Fig. 1 was manually printed on the surface of the SE and then heated in air at 250 °C for 20 min, which mainly served to collect current and weld the Pt wire. Compared with Pt paste, Ag paste has little effect on the sensitivity test and is inexpensive. The sensor was wholly exposed to base gas containing 10 vol.% O_2 or to different NO concentrations.
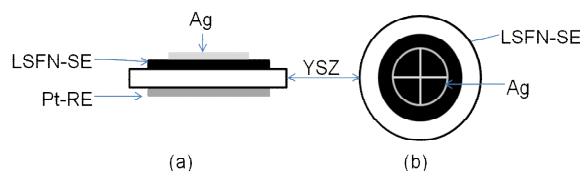

Fig.1 The schematic of the NOx sensor (a) side view, (b) top view.

Characterization. The crystal structure of the powder and SE were examined by XRD (X'Pert PRO, PANalytical B.V., Holland) with Cu-kα radiation. Their surface morphologies were determined by ESEM (Quanta200, FEI, Holland) with an excitation voltage of 20kV.

Evaluation of Sensor Properties. Details and schematics of the experimental setup have been given previously [22]. Pt wires were attached to both electrodes to collect signals and soldered with Ag paste. The difference of electric potentials (V) between the sensing and reference electrode was monitored and recorded using an electrochemical workstation (VersaSTAT 3, Princeton, USA). The sensor was alternatively exposed to a base gas (10 vol. % O_2, N_2 balance) and an NO sample gas (100–800 ppm in 10 vol. % O_2, N_2 balance) at a total flow rate of 200 ml/min between 300 to 550 °C.

TPD Procedure. The NO adsorption-desorption behavior of sensitive material was measured using an automated chemical adsorption instrument (AutoChem II2920; Micromerities, USA). The adsorption gas concentration is 2000 ppm NO, balanced with He. A 50 mg powder sample calcined at 800 °C was supported on a quartz cotton sheet of a U-shaped quartz tube reactor. Prior to the experiment, the sample was pretreated at 700 °C in a mixture of 4 % oxygen balanced by He flowing to ensure consistent lattice oxygen content and to remove any surface contaminants. Then, sample was cooled to 300 °C at 30 °C /min under the same gas flow as the pretreatment. Once the sample reached 300 °C, the adsorbing gas was flowed over the sample for 30 min, followed by cooling to 50 °C at 5 °C /min under the same gas flow. Below 50 °C, the gas was switched to He and allowed to

equilibrate for 16 h. Once equilibrated, the sample was heated at 30 °C /min to 600 °C in He and the desorbed gas effluent was measured using an Extrel quadrupole mass spectrometer (MS). All gases were flown at the same rate of 25 ml/min.

Results and Discussion

SE Microstructure. The XRD data show that the LSFN powder calcined at 800 °C has a perovskite structure, cubic symmetry. Lattice parameters *a*, *b*, *c* are 0.387 nm, and the interplanar spacing *d* corresponding to the strongest peak is 0.274 nm (Fig. 2 (a)). Compared with the LSFN powder, the XRD diffraction peak of the SE sintered at 1300 °C shifted slightly to the left. It is shown that the interplanar spacing of the SE is slightly increased under the influence of temperature, and the intensity of all diffraction peaks became weaker, but the structure was consistent, which was a good pure perovskite phase (Fig. 2 (b)). Lattice parameters are slightly increased to 0.398 nm, and the *d* value corresponding to the strongest peak becomes 0.275 nm. The main phase ZrO_2 in YSZ also has a cubic symmetry structure, as shown in Fig. 2 (c).

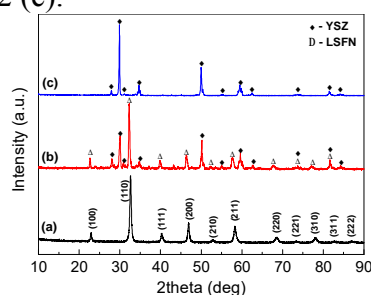Fig.2 XRD patterns of (a) LSFN powder , (b) LSFN（sintered at 1300 ℃）+YSZ and (c)YSZ.

Fig.3 shows micrographs of the surface morphology of the LSFN powder and SE. The powder consists of uniform and fine spherical particles. Particle size distribution range of the powder is about 80-90 nm. The agglomerates of the particles are observed in the image of Fig.3(a).The LSFN-SE particle size distribution range is about 0.6-0.8 μm. Obviously, as the sintering temperature increases, the particles grow, and also it could be found that the sintering necks were formed between the grains. The agglomerations of the particles were also observed in the local area of the SE. As exhibited in Fig.3(b), the LSFN-SE shows a porous structure, which is conducive to the gas quickly through the SE layer to reach the triple-phase boundary (TPB) of YSZ, LSFN-SE and NO gas.
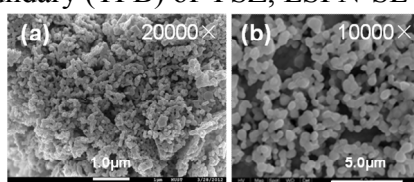

Fig.3 SEM images of (a) LSFN powder calcined at 800 °C, (b) LSFN-SE sintered at 1300 °C.

NO Sensitivity of (Ag)LSFN/YSZ/Pt Sensor. The sensitivity to 600 ppm NO is measured in 10 vol.% O_2 with N_2 balance in the temperature range of 300-550 °C (Fig. 4). With the increase of operating temperature, the response value is gradually reduced, the response is negative. The maximum response value is obtained at 300 °C, about -78 mV. Obviously, the response rate is faster than the recovery rate at the same operating temperature. As the temperature increases, the response and recovery times are reduced in turn, and the recovery time changes significantly with the change of temperature.
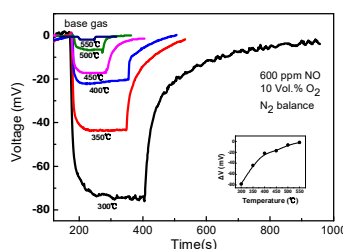
Fig.4 The sensor with LSFN-SE sintered at 1300 °C in different temperature of the response transients to 600 ppm NO (The inset is the corresponding response potential value).

Fig.5 shows the transient response of the sensor with 1300 °C-sintered LSFN-SE at 300, 350 and 400 °C for different NO concentrations. With the increase of NO concentration, the response potential increases in turn, and the response potential is linearly related to the logarithm between 100-800 ppm NO concentration and the slope at 300 °C is -8.65 mV / decade.
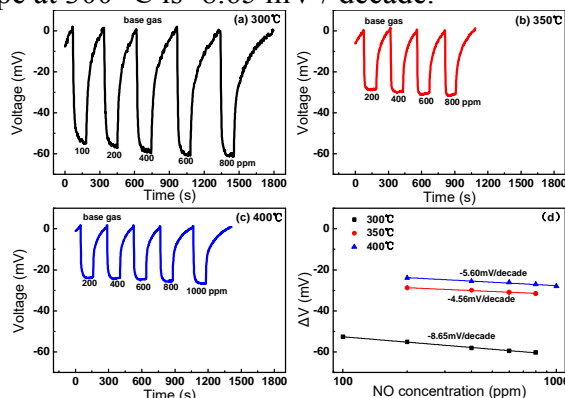

Fig.5 The sensor in different temperatures of the response transients to different concentrations of NO （a）300 °C, （b）350 °C, （c）400 °C and（d）the relationship between NO concentration and potential.

Fig.6 shows the response repeatability test of the sensor at 300, 350 and 400 °C for 600 ppm NO. It can be seen that the sensor has good response repeatability.
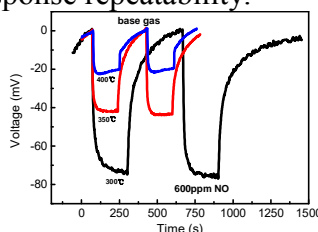

Fig.6 Repeated response transients of sensor to 600 ppm NO in 300, 350 and 400 °C.

Fig. 7 shows that the LSFN powder has only physical desorption of NO, and the Tm (Tm represents the peak temperature at which the desorption rate is maximum) corresponding to desorption is 106 °C. After this temperature, NO desorption rate decreases as the temperature increases. Desorption of NO was not observed at substantially above 300 °C. Therefore, it should be noted here that the conditions of the TPD measurement are very different from the sensor operating conditions. Although NO gas is swept from the oxide sample by He gas in the TPD measurement, the oxide SE of the sensor is always exposed to the NO gas during the sensor operation. This can explain the result that the NO sensitivity was obtained where any NO desorption peak was not observed in the TPD measurement. The result of no desorption peak observed above 300 °C indicated that the NO adsorption on the LSFN was weak. This may lead to the low catalytic activity for the cathodic reaction (1). So its sensitivity to NO was small. In a certain concentration of NO atmosphere, increasing the temperature and increasing molecular thermal motion will reduce the amount of adsorption NO and shorten the residence time on the SE, thereby reducing the potential response and sensitivity, while making the response rate and recovery rate faster, especially the recovery rate [25]. This law coincides with the decrease in NO with the temperature rise and the response and recovery becomes faster in this study.

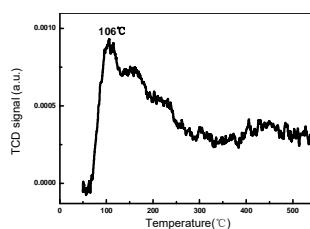$$2NO + 2O^{2-} \rightarrow 2NO_2 + 4e^- \tag{1}$$
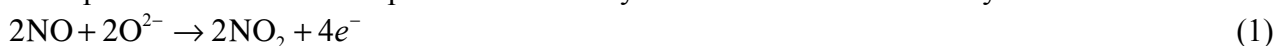
Fig.7 The TPD curve of NO for the LSFN powder calcined at 800 °C.

Conclusions

(1) Between 300 to 550 °C, the potential response value of the sensor to 600 ppm NO decreases with the increase of temperature, and the largest response (about -78 mV) is achieved at 300 °C, the response and recovery rates are increased in turn, especially the recovery rate.

 (2) In the range of 100-800 ppm NO concentration, the logarithm of concentration is linear relationship with the response potential, and the slope is the highest at 300 °C, which is -8.65 mV / decade.

 (3) Tests of 600 ppm NO at 300, 350 and 400 °C indicate that the sensor has good reproducibility.

 (4) TPD result of the LSFN oxide indicates any desorption peak of NO is not observed above 300 °C. The weak NO adsorption-desorption behavior of LSFN may result in a small sensitivity to NO.

Acknowledgements

References

[1] J. Park, B.Y. Yoon, C.O. Park, W.J. Lee and C.B. Lee: Sens. Actuators B. Vol. 135 (2009), p. 516

[2] Q. Diao, C. Yin, Y. Guan, X. Liang, S. Wang, Y. Liu, Y. Hu, H. Chen and G. Lu: Sens. Actuators B. Vol. 177 (2013), p. 397

[3] J.M. Rheaume and A.P. Pisano: Ionics Vol. 17 (2011), p. 99

[4] S. Fischer, R. Pohle, B. Farber, R. Proch, J. Kaniuk, M. Fleischer and R. Moos: Sens. Actuators B. Vol. 147 (2010), p. 780

[5] F. Ménil, V. Coillard and C. Lucat: Sens. Actuators B. Vol. 67 (2000), p. 1

[6] L.Y. Woo, R.S. Glass, R.F. Novak and J.H. Visser: Sens. Actuators B. Vol. 157 (2011), p. 115

 [7] S. Zhuiykov and N. Miura: Sens. Actuators B. Vol. 121 (2007), p. 639

[8] V.V. Plashnitsa, P. Elumalai, Y. Fujio and N. Miura: Electrochim. Acta. Vol. 54 (2009), p. 6099

[9] E.R. Macam, B.M. Blackburn and E.D. Wachsman: Sens. Actuators B. Vol. 158 (2011), p. 304

[10] E. Di Bartolomeo, M.L. Grilli and E. Traversa: J. Electrochem. Soc. Vol. 151 (2004), p. H133

[11] V.V. Plashnitsa, V. Gupta and N. Miura: Electrochim. Acta. Vol. 55 (2010), p. 6941

[12] J. Yoo, S. Chatterjee and E.D. Wachsman: Sens. Actuators B. Vol. 122 (2007), p. 644

[13] N. Miura, K. Akisada, J. Wang, S. Zhuiykov and T. Ono: Ionics Vol. 10 (2004), p. 1

[14] J. Yoo and E.D. Wachsman: Sens. Actuators B. Vol. 123 (2007), p. 915

[15] K. Mahendraprabhu and P. Elumalai: Sens. Actuators B. Vol. 238 (2017), p. 105

[16] S. Zhuiykov, T. Nakano, A. Kunimoto, N. Yamazoe and N. Miura: Electrochem. Commun. Vol. 3 (2001), p. 97

[17] N. Miura, S. Zhuiykov, T. Ono, M. Hasei and N. Yamazoe: Sens. Actuators B. Vol. 83 (2002), p. 222

[18] S. Zhuiykov, T. Ono, N. Yamazoe and N. Miura: Solid State Ion. Vol.152 (2002), p. 801

[19] J.W. Yoon, M.L. Grilli, E.D. Bartolomeo, R. Polini and E. Traversa: Sens. Actuators B. Vol. 76 (2001), p. 483

[20] E.R. Macam, B.M. Blackburn and E.D. Wachsman: Sens. Actuators B. Vol. 157 (2011), p. 353

[21] Y. Chen and J. Xiao: Sens. Actuators B. Vol. 192 (2014), p. 730

[22] L. Zhou, X. Li, H. Wu, Z. Liao, Q. Yuan, F. Xia and J. Xiao: Ceram. Int. Vol. 40 (2014), p. 9257

[23] L. Zhou, Q. Yuan, X. Li, J. Xu, F. Xia and J. Xiao: Sens. Actuators B. Vol. 206 (2015), p. 311

[24] F. Liu, B. Wang, X. Yang, Y. Guan, Q. Wang, X. Liang, P. Sun, Y. Wang and G. Lu: Sens. Actuators B. Vol. 240 (2017), p. 148

[25] R. Moos: Sensors. Vol. 10 (2010), p. 6773